



Pseudomonas aeruginosa quorum sensing and biofilm attenuation by a di-hydroxy derivative of piperlongumine (PL-18)

Yael Schlichter Kadosh^{a,1}, Subramani Muthuraman^{b,1}, Khairun Nisaa^c, Anat Ben-Zvi^c, Danit Lisa Karsagi Byron^d, Marilou Shagan^a, Alexander Brandis^e, Tevie Mehlman^e, Jacob Gopas^f, Rajendran Saravana Kumar^{b,**}, Ariel Kushmaro^{a,g,h,*}

^a Avram and Stella Goldstein-Goren Department of Biotechnology Engineering, Ben Gurion University of the Negev, Beer Sheva, Israel

^b Chemistry Division, Vellore Institute of Technology, Chennai, India

^c Department of Life Science, Ben-Gurion University of the Negev, Beer Sheva, Israel

^d Department of Civil and Environmental Engineering, Ben-Gurion University of the Negev, Beer Sheva, Israel

^e Department of Life Sciences Core Facilities, Weizmann Institute of Science, Rehovot, Israel

^f Department of Microbiology, Immunology and Genetics Faculty of Health Sciences, Ben Gurion University of the Negev, Beer Sheva, Israel

^g The Ilse Katz Center for Nanoscale Science and Technology, Ben Gurion University of the Negev, Beer Sheva, Israel

^h School of Sustainability and Climate Change, Ben Gurion University of the Negev, Beer Sheva, Israel

ARTICLE INFO

Keywords:

Piperlongumine
Piper longum
Amide alkaloid
Pseudomonas aeruginosa
Quorum sensing
Bacterial biofilm
Iron acquisition
Transcriptome

ABSTRACT

Bacterial communication, Quorum Sensing (QS), is a target against virulence and prevention of antibiotic-resistant infections. 16 derivatives of Piperlongumine (PL), an amide alkaloid from *Piper longum* L., were screened for QS inhibition. PL-18 had the best QSI activity. PL-18 inhibited the *lasR-lasI*, *rhlR-rhlI*, and *pqs* QS systems of *Pseudomonas aeruginosa*. PL-18 inhibited pyocyanin and rhamnolipids that are QS-controlled virulence elements. Iron is an essential element for pathogenicity, biofilm formation and resilience in harsh environments, its uptake was inhibited by PL-18. PL-18 significantly reduced the biofilm biovolume including in established biofilms. PL-18-coated silicon tubes significantly inhibited biofilm formation. The transcriptome study of treated *P. aeruginosa* showed that PL-18 indeed reduced the expression of QS and iron homeostasis related genes, and up regulated sulfur metabolism related genes. Altogether, PL-18 inhibits QS, virulence, iron uptake, and biofilm formation. Thus, PL-18 should be further developed against bacterial infection, antibiotic resistance, and biofilm formation.

1. Introduction

Bacterial resistance to antibiotics is of important worldwide concern. Conventional antibiotics that kill bacteria very often lead to the development of resistance [1,2]. However, there have been fewer and fewer new antibiotics developed and approved for many years. Without new antibiotics, we are facing the post-antibiotic era, in which health providers will be unable to prevent or treat bacterial infections. Therefore, new approaches to combat bacterial infections should be considered [3–5].

As an alternative to the conventional antibiotic killing of bacteria, a process that may result in the selection of resistant strains, the

development of compounds that attenuate bacterial virulence and prevent pathogenicity should be pursued. One important target for such attenuation is the use of Quorum Sensing (QS) as a target. QS controls gene expression in response to changes in bacterial concentration. This occurs by the production and secretion of Auto-Inducers (AI). When the population density is low, the AI released by the bacteria quickly becomes diluted by diffusion. However, as the population grows, the AI concentration is increased beyond a certain threshold, which then activates specific gene expression in order to achieve maximum efficiency [6]. This phenomenon is especially relevant to the expression of virulence factors that increase their effectiveness. The AI signal molecules in Gram-negative bacteria include but are not limited to variants of

* Corresponding author. Avram and Stella Goldstein-Goren Department of Biotechnology Engineering, Ben Gurion University of the Negev, Beer Sheva, Israel.

** Corresponding author.

E-mail addresses: sar.org@gmail.com (R. Saravana Kumar), arielkus@bgu.ac.il (A. Kushmaro).

¹ Equal contribution.

Homo-Serine Lactones (HSL). The variants are a result of differences in the length of the carbon chain (4–18 carbons), the saturation level, and the oxidation state at the C3 position [7]. These AIs are the ligands of LuxR receptor family.

Pseudomonas aeruginosa is a model for a gram-negative opportunist pathogen. This bacterium commonly causes infection in hospital environments and immunosuppressed individuals. Some strains are multidrug-resistant (MDR) [8,9]. *P. aeruginosa* expresses many virulence factors resulting in antibiotic resistance and biofilm formation as well as secretion of toxins, lipases, pyocyanin, rhamnolipids, siderophores, and proteases. *P. aeruginosa* has two LuxR types of QS systems: LasI/LasR, and RhlI/RhlR responsive to the AI 3-oxo-C12-HSL and C4-HSL, respectively [10,11]. Deletion of the QS genes in *P. aeruginosa* causes a decrease or elimination of virulence behaviors [12–14]. *P. aeruginosa* utilized a third QS system-based on the compound 2-heptyl-3-hydroxy-4-quinolone named Pseudomonas Quinolone Signal (PQS). The pqs system is also important for biofilm formation, pyocyanin synthesis, and other virulence activities [15]. The three QS systems are separate but are interconnected with distinct hierarchy [16].

P. aeruginosa and many other bacteria develop biofilms that are characterized by adherence of the bacteria to a surface, and by the formation of bacterial extracellular matrix (ECM). Biofilm formation is a major problem in healthcare systems due to its stability even under stressful environmental challenges, including oxidative stress, the presence of antibiotics, and the host immune response [17]. Indeed, biofilms on medical devices (e.g., implants and catheters) may be chronic and can cause their failure [18]. Biofilm of *P. aeruginosa* in Cystic Fibrosis patients' lungs and on burn victim tissues, were found to be stable and to cause persistent infections that lead to severe chronic inflammation [19,20].

Many plants secondary metabolites are essential for plant protection against microbial pathogens. These compounds have long been considered an important source for drug discovery [21,22]. The synthesis of new derivatives of these metabolites increases the probability of finding new drugs for many therapeutic purposes. The derivatives of these metabolites may display new biological activities, absent in the original natural product or enable the modulation of the original activities (e.g., solubility, reactivity, and specificity). Moreover, such variants are useful to study basic and applied questions related to their mode of action and the role of different chemical functional groups.

Piperlongumine (PL) is an amide alkaloid isolated from *P. longum* L. (Long pepper) and the synthesis of its derivatives has been described in previous works [23,24]. Long pepper has long been used in traditional medicine. Known to be beneficial in treating many illnesses including cancer, inflammation, depression, diabetes, obesity, and hepatotoxicity [25]. PL has multiple biological activities such as anti-platelet aggregation, anti-anxiolytic and anti-depressant [26]. PL is mainly known as an anti-cancer agent which selectively inhibits cancerous cells [27]. PL was shown to directly inhibit the Nuclear Factor kappa B (NF- κ B) pathway by interacting with I κ B Kinase (IKK) and elevation of Reactive Oxygen Species (ROS) [28,29]. It also moderately inhibits bacterial and fungal growth [30]. Since their effect on QS has not previously been studied, here we investigated the QS Inhibitory (QSI) activity of PL and its derivatives. Piperlongumine and its derivatives are small molecules, similar to other effective QSI molecules, such as halogenated furanone [31] and hordenine analogs [32]. The objective of this study, therefore, is to investigate Piperlongumine (PL) and its derivatives activity as non-antibiotic QS inhibitors.

2. Materials and methods

2.1. Synthesis of PL derivatives

PL required for the present study was isolated from long pepper, it was sequentially modified i.e., demethylation to obtain monohydroxy

piperlongumine (PL-07), dihydroxy piperlongumine (PL-18), and trihydroxy piperlongumine (PL-25) Subramani et al. (2020) [23]. The other PL derivatives, PL-17,20, 23B, AE-02, 04, 11, 17, 45, 68, 73 and 77 were prepared by transamidation of PL with corresponding amines as previously described by Muthuraman et al. (2019) [33]. AE-10 was synthesized by transamidation of PL-07 with ethyl amine. PL-31 was synthesized as reported earlier by Muthuraman et al. (2019) [24]. The derivatives are listed in Table 1, and details of the synthesis and validation are in Supplementary file 2.

2.2. Screening of QSI activity

Two bio-reporter bacteria *Chromobacterium violaceum* (CV026) and *Agrobacterium tumefaciens* (KYC55) were used for the detection of AI [34, 35], and for the detection of multiple QSI molecules in parallel [36] as described before. These bacteria were used to determine the QSI activity of the PL derivatives listed in Table 1. Briefly, the compounds dissolved in acetonitrile (Sigma-Aldrich, MO, USA) to 40 mM, and 20 μ L were positioned and dried on the same spot on Thin-Layer chromatography membrane (TLC, Merk, Darmstadt, Germany). Then, CV026 or KYC55 cultures were mixed with the AI: 500 nM of 3-oxo-C6 (K3007), and of 3-oxo-c8 (O1764) (both from Sigma-Aldrich), respectively. Since these two reporter bacteria are null mutants of the synthetase gene, they can't produce the AI endogenously. In addition, 60 μ g/mL Xgal (Sigma Aldrich) was added to KYC55. The cultures were placed on top of the TLC and incubated at 30 °C for 24 h. The effect of the derivatives on the culture's color was assessed qualitatively. Representative images from the experiment are presented in Supplementary Fig. 1.

2.3. QS receptors of *P. aeruginosa* activation by a bioluminescence reporter assay

PAO-JP2-luxCDABE LasR antagonist assays were performed as described previously by Ganin et al. (2009) [37]. PAO-JP2, a lasI-rhlI double mutant of PAO1, harbored a plasmid pKD201 with a lasI promoter coupled to the luxCDABE operon. PAO-JP2-luxCDABE starter culture in LB (Difco Lenox medium, BD, France) with 300 μ g/mL trimethoprim (TMP, Sigma-Aldrich) was incubated for 24 h, shaking at 37 °C, and then diluted (1:5). AI was added to a final concentration of 100 nM of 3-oxo-C12-HSL (O9139, Sigma-Aldrich). A 96-well white/clear bottom microtiter plate (Greiner Bio-One, Kremsmunster, Austria) was prepared with the desired concentrations of PL-18 as indicated in Fig. 1 a. PL-18 was dissolved and diluted in DMSO (Sigma-Aldrich). The control group's DMSO concentration was equal to the tested groups. The DMSO concentration was always lower than 0.5 %. The plate was then incubated for 10 h at 37 °C, and during this time luminescence measurements were performed at 15 min intervals using a luminometer (Varioskan Flash, Thermo Fisher Scientific, MA, USA).

PAO-JP2 (pKD-rhlA) is a reporter strain that measures RhlR activity, developed by K. Duan et al. (2007) [38]. The rhlA promoter, responsive to RhlR-C4-HSL, was fused upstream to the luxCDABE box and introduced into PAO-JP2. The starter culture was grown in LB with 300 μ g/mL TMP for 24 h, shaking at 37 °C, then diluted (1:5). The AI was added to a final concentration of 10 μ M of C4-HSL (SML3427, Sigma-Aldrich). A 96-well white/clear bottom microtiter plate was prepared with the desired concentrations of PL-18 as indicated in Fig. 1 b. The plate was then incubated for a period of 10 h at 37 °C, and during this time luminescence measurements were performed at 15 min intervals using a luminometer.

The same bioluminescence method was used to determine the effect of iron concentration on PL-18 QSI activity, in the presence of the iron chelator ethylenediamine-N,N'-bis(2-hydroxyphenylacetic acid), (EDDHA, AS060816, Arctom Scientific, CA USA). PL-18 and EDDHA were added in a combinatory manner as described in Supplementary Fig. 9.

PAO1- Δ pqsAH-CTXlux-pqsA reporter strain was developed by P. Williams et al. (2014) [39,40], to determine the PqsR receptor activity. The strain starter culture was grown in LB in the presence of 125 μ M tetracycline (Sigma-Aldrich) at 37 °C, overnight. Then diluted to 0.04 O.D. at 600 nm and grown to an O.D. between 0.2 and 0.4. 25 μ M of Heptyl-3-hydroxy-4(1H)-quinolone (PQS, 94398, Sigma-Aldrich) was then added to the culture. Then 180 μ L of the cultures were placed in the wells of a 96-well white/clear bottom microtiter plate that was prepared with the desired concentrations of PL-18 in 20 μ L as indicated in Fig. 1 c, to a final volume of 200 μ L. The plate was then incubated for a period of 15 h at 37 °C, and during this time luminescence measurements were performed at 15 min intervals using a luminometer.

2.4. Ligand-binding domain of the LasR (LasR-LBD) expression and purification

The expression and purification of the LasR-LBD his-tag protein was previously published by us [41]. Briefly, the construct was expressed in *E. coli* BL21-pETM-11 in the presence of isopropyl β -D-1-thiogalactopyranoside (IPTG, Sigma-Aldrich), 160 μ M PL-18 or DMSO, with or without 3-oxo-C12-HSL. Then bacteria were separated from the supernatant by centrifugation and lysed, followed by additional centrifugation of the lysate. The soluble fraction was then loaded on a nickel-affinity chromatography for purification. The detection of LasR-LBD was by Western blot. Samples were taken from the elution and mixed with sample buffer (GenScript, A₂S technologies, Yavne, Israel) and heated at 95 °C for 5 min before loading onto 12 % acryl amid SDS-PAGE (37.5:1 acrylamide/bisacrylamide, Bio-Lab, Israel). The membrane was blocked with 5 % bovine serum albumin (Roth, A₂S technologies), and was incubated with primary antibody mouse Anti-6X His tag® antibody (ab49936, Abcam, Cambridge, UK) followed by a secondary antibody anti-mouse IgG Horse Radish Peroxidase-linked antibody (7076S, Cell Signaling technology, MA, USA). Chemiluminescence was detected (Azure Biosystems 400, CA, USA).

2.5. Quantification of virulence factors from the cell-free culture supernatants of *P. aeruginosa*

P. aeruginosa (PAO1) starter culture was grown overnight and then diluted (1:10) in LB broth. PL-18 or DMSO were added to the culture and incubated in a shaker for 24 h at 37 °C. Cells were harvested by centrifugation and the supernatants were collected and filtered through 0.22 μ m into fresh tubes. To measure the pyocyanin presence in the supernatant, it was extracted using the chloroform-HCl method and read at 520 nm in a plate-reader UltrospecPro spectrophotometer (GE Healthcare, Little Chalfont, UK). Determination of rhamnolipids content was measured at 570 nm directly from the cell-free supernatant after adjustment to pH 2 [42]. Elastase activity was then measured at 400 nm by adding to the filtered supernatant elastin-Congo-red (Sigma-Aldrich) at 37 °C, 140 rpm agitation for 16 h [43].

2.6. *P. aeruginosa* swarming motility assay

The *P. aeruginosa* (PAO1) swarming motility test was described before by Yehuda N. et al. (2022) [44]. Briefly, PAO1 was grown overnight in M9 medium. Then diluted 1:10 in M9 medium and incubated at 37 °C until it reached 0.4–0.6 O.D. at 600 nm. 1 μ L of the culture was placed in the middle of the 0.5 % agar M9 plates that contained PL-18 or DMSO in concentrations indicated in Supplementary Fig. 1 a. Followed by incubation for 24 h at 37 °C. The assessment of the surface coverage was done in ImageJ by applying a threshold, transforming the images to binary, and determining the area of the bacteria.

2.7. *P. aeruginosa* growth and viability response to PL-18

The growth of PAO1 bacteria was determined using kinetic measurements of O.D. (600 nm). An overnight culture of PAO1 was diluted (1:100) in LB broth and combined with increasing concentrations of PL-18 or DMSO. The measurements were done in 20 min intervals for 10 h, medium shaking, at 37 °C in a plate reader (Multiskan Go, Thermo Fisher Scientific). The viability of PAO1 after 24 h with PL-18 was determined by CFU counting. An overnight culture of PAO1 was diluted (1:100) in LB broth and combined with increasing concentrations of PL-18 or DMSO. The tested cultures were incubated for 24 h, shaking at 37 °C. After, each tested culture was serially diluted and Sown for CFU counting on LB-agar Petri dishes. PL-18 concentration is indicated in Supplementary Fig. 5 a, and b.

2.8. Iron quantification by inductively coupled plasma optical emission (ICP-EOS) spectrometry

In order to determine the effect of PL-18 on iron uptake by *P. aeruginosa* (PAO1), iron concentration was measured by ICP-EOS. PAO1 starter cultures were centrifuged and washed with Phosphate Buffered Saline (PBS, Biological Industries, Israel) before it was incubated in LB with 160 μ M PL-18 or DMSO for 7 h. Pellets and supernatants were separated by centrifugation. The supernatant was filtered through 0.22 filters (pre-washed with LB) and transferred to glass vials that were pre-washed with 20 % (v/v) HNO₃. The pellets were washed once by adding Ultra-Pure Water (UPW, Bio-Lab), centrifuged, then suspended in UPS, and transferred to glass vials, also pre-washed with 20 % HNO₃. The samples were dried at 51 °C for 48 h followed by mineralization by incubation in 68 % HNO₃ for 24 h at RT. Then the volume was brought to 10 mL with UPW and filtered through 0.45 μ m that was pre-washed with 5 % HNO₃ [45]. Iron concentration was measured by ICP-EOS (SPECTRO ARCOS ICP-OES analyzer).

2.9. Confocal laser scanning microscopy (CLSM) for *P. aeruginosa* biofilm visualization and quantification

Biofilm biovolume was determined using continuous-culture flow cells [46]. The overnight PAO1 culture in LB broth was diluted to an O.D. of 0.1 (600 nm) in PBS. 400 μ L of the diluted culture was incubated for 1 h at 30 °C. The flow cell ran at a rate of 3 mL/h (Masterflex L/S peristaltic pump (Cole-Parmer, Vernon Hills, IL, USA) in AB minimal medium. The biofilm in Fig. 3 a and b was grown in a μ -Slide VI 0.4 Uncoated (© ibidi GmbH, Grafelfing, Germany) for 72 h at 30 °C. in the presence of PL-18 (10, 40 μ M) or DMSO. Before establishing the biofilm in Fig. 3 c and d, PL-18 was dissolved in chloroform at 10 mM. 40 μ L were dried twice on the inner surface of 3.5 cm segments of silicone tubes (ISMATEC™, 1.02 mm). PAO1 was grown as a biofilm inside the untreated, chloroform or PL-18 treated silicone tubes for 72 h at 30 °C. The biofilm in Fig. 3 e and f, grew in μ -Slide VI 0.4 Uncoated at 30 °C for 24 h. Then, 40 μ M PL-18 or DMSO were added to the medium, and the biofilm grew for an additional 24 h.

Bacterial viability in the biofilm was determined using a LIVE/DEAD™ BacLight™ (Invitrogen, Eugene, OR, USA) staining kit according to the manufacturer's instructions. The biofilms were washed before and after the staining with PBS. Z-stack imaging was acquired by the CSLM, (FV1000, Olympus, Tokyo, Japan), at 63 \times magnification. SYTO 9 dye was excited by a 488 nm laser and emission was collected at 515 nm. For the red-dead Propidium Iodide, excitation was at 530 nm and emission was recorded at 617 nm. 3D visualization and biofilm volume calculation were processed using IMARIS software (Bitplane AG, Zurich, Switzerland). The biovolume was normalized to the area of the image. After staining, the biofilms in the silicon tubes were fixed with Paraformaldehyde 4 % for 20 min at RT, then were sliced and attached to

glass using mounting oil, to be observed by CLSM at 10× magnification. 80 Z planes (each Z plane was 0.5 μM) were included in the final image.

2.10. Scanning Electron Microscope (SEM) analysis of coated silicon tubes

The presence of PL-18 crystals on coated tubes was assessed by High Resolution SEM (HR-SEM) imaging. PL-18 was dissolved in chloroform at 10 mM. 40 μL were dried twice on the inner surface of 3.5 cm segments of silicone tubes. Then untreated, chloroform or PL-18 treated tube segments were attached to the flow system and AB medium was allowed to flow for 5 min and 30 min. Control tubes (no flow) and tubes under flow were sliced and attached to a specimen holder with double-side carbon tape and coated with a 20 nm layer of gold using an EMI-TECH K575x sputtering device (Emitech Ltd., UK). Imaging was done at SEM.

2.11. RNA extraction

In order to perform the transcriptome analysis and RT-qPCR validation to determine the effect of PL-18 on gene expression, RNA was extracted as follows: PAO1 bacteria were grown overnight and then diluted (1:10) in 2 mL LB broth. 160 μM PL-18 or DMSO were added to the culture and incubated in a shaker for 7 h at 37 °C. 500 μL of each culture was transferred to a new tube and mixed with RNAprotect Bacteria Reagent (QIAGEN GmbH, Hilden, Germany) for 5 min. Cells were harvested by centrifugation and the supernatant discarded. Bacterial lysis and RNA isolation were performed with the RNeasy mini kit (QIAGEN) with the addition of Tris-EDTA buffer solution pH 8.0, Proteinase K from *Tririrachium album*, and lysozyme from chicken egg white (all purchased from Sigma-Aldrich) as determined by the manufacturer. On-column DNA digestion was performed with the RNase-free DNase SET (QIAGEN). RNA was eluted in UPW.

2.12. Transcriptome analysis- RNA sequencing

For transcriptome analysis, RNA was sequenced by Illumina. Total RNA was processed for an additional DNase treatment using a RNase-Free DNase kit (Qiagen; ID: 79254). DNase-treated RNA was purified using the RNeasy MinElute Cleanup kit (Qiagen; ID: 74204). Both steps were automated on a QIAcube instrument according to the manufacturer's instructions. Ribosomal RNA depletion was performed using a bacterial QIAseq FastSelect rRNA depletion kit Qiagen; (ID: 335927) according to the manufacturer's instructions. Ribosomal RNA-depleted RNA was then used as a template for library preparation using a NEXTFLEX® Rapid Directional RNA-Seq Kit 2.0 (PerkinElmer) with adapters containing unique dual indices (UDIs). Libraries were evaluated for quality using a small sequencing run on an Illumina MiniSeq with a mid-output flow cell (2x150 base sequences). Libraries were re-pooled and deeply sequenced on an Illumina NovaSeq6000 instrument using an SP flow cell with 2x150 base sequencing. DNase treatment, rRNA depletion, library preparation and QC sequencing were performed at the Genomics and Microbiome Core Facility (GMCF) at Rush University. Illumina NovaSeq6000 sequencing was performed at the DNA Services Lab at the University of Illinois at Urbana-Champaign.

2.13. Transcriptome analysis-bioinformatics

The processes of raw sequence reads were performed before [47] [ref DIM] and the results are presented in Supplementary Table 1 Excel sheet 1. Genes were considered differentially expressed if they had FDR-adjusted *p*-value <0.05 and absolute fold change (in linear scale) ≥ 1.3. Pathway enrichment in the Kyoto Encyclopedia of gene and genome (KEGG) was used for sulfur metabolism and biofilm formation of *P. aeruginosa* [48–50]. Clustering and STRING network were prepared in the Cytoscape software and the STRING database. Analysis was

performed on genes at the cut off of ±2 FC. Default parameters were used in the analysis.

2.14. Validation of gene expression by RT-qPCR

To validate the transcriptome results, the relative gene expression of representative genes was tested using RT-qPCR. RNA concentration and quality were determined by NanoDrop™ One/OneC Microvolume UV-Vis Spectrophotometer (Thermo Fisher Scientific). RNA was converted into cDNA using the PrimeScriptRT Master Mix (Perfect Real Time, Takara-Clontech) following the manufacturer's instructions. Subsequently, the qPCR reaction was prepared using the pre-mixed qPCR BIO SyGreen Blue Mix Hi-ROX (PCR Biosystems, PA, USA), the primers listed in Supplementary Table 1 Excel sheet 3, and 5 μL of the RNA sample to a final volume of 20 μL. The StepOne™ Real-Time PCR System instrument (Thermo Fisher Scientific) was used. An initial denaturation-hot start of 15 min at 95 °C was followed by 40 cycles of the following incubation protocol: 94 °C for 15 s, 60 °C for 60 s. The procedure was completed with a final elongation step of 1 min at 95 °C. The relative gene expression was calculated by $-2^{-\Delta\Delta Ct}$; $\Delta Ct =$ The Ct of a target gene in the treatment group was subtracted from the Ct of a housekeeping gene (*proC*). $\Delta\Delta Ct =$ the ΔCt of the treatment group was subtracted from the ΔCt of the control group. In the graph (Fig. 5 b), $-2^{-\Delta\Delta Ct}$ was plotted. The Gene code for the identification of the genes was obtained from the Pseudomonas database [51] (<https://www.pseudomonas.com/>).

2.15. Cyclic- Di-GMP quantification

P. aeruginosa culture was diluted 1:10 in LB with DMSO or PL-18 at 40 or 160 μM and incubated with shaking for 7 h, at 37 °C. For sample preparation, c-di-GMP was extracted with PBS at 100 °C and then with 65%-ethanol and vacuum-dried according to the procedure of Roy et al., 2013 [52]. 15N5-adenosine 5'-monophosphate at 0.5 mM (15N5-AMP, Sigma) was added to standards and samples as internal standard. The dried extracts were resuspended in 100 μL of nano-pure water, vortexed for 1 min, and centrifuged (21,000×g, 5 min) to remove insoluble material. The obtained supernatant was placed in LC-MS vials for analysis.

For the analysis, the LC-MS/MS instrument consisted of an Acquity I-class UPLC system (Waters) and Xevo TQ-S triple quadrupole mass spectrometer (Waters) equipped with an electrospray ion source and operated in positive ion mode using analysis. MassLynx and TargetLynx software (v.4.2, Waters) were applied for the acquisition and analysis of data. Chromatographic separation was done on a 50 x 2.1-mm i.d. 1.7-μm UPLC BEH C18 column (Acquity, Waters) with 20 mM ammonium formate, pH3 as mobile phase A and acetonitrile as mobile phase B, at a flow rate of 0.3 mL/min and column temperature 25 °C. A gradient was as follows: for 1 min, the column was held at 0%B, then linear increase to 100%B in 4 min, then back to 0%B in 1 min, and equilibration at 0%B for 2 min. Samples kept at 8 °C were automatically injected in a volume of 1 μL.

For mass spectrometry, Argon was used as the collision gas with a flow of 0.10 mL/min. The capillary voltage was set to 3.00 kV, cone voltage 30 V, source temperature 150 °C, desolvation temperature 350 °C, desolvation gas flow 650 L/h, cone gas flow 150 L/h. Analytes were detected using corresponding retention time and selected reaction monitoring (SRM) for single and double charged precursor ions (collision energy CE, eV): 691.0 > 540.0 (21), 691.0 > 152.0 (27) *m/z*, and 346.0 > 540.0 (9), 346.0 > 152.0 (9) *m/z*, respectively. SRM for 15N5-AMP: 353.1 > 141.1 (20) *m/z*.

Quantification was made using a standard curve in the 0–10 mM concentration range with 3',3'-c-di-GMP (InvivoGen). ¹⁵N5-adenosine 5'-monophosphate (Sigma) was added to standards and samples as internal standard (0.5 mM). The peak areas of the respective mass fragments from single and double charged precursor ions) were summarized as described by Bahre et al., 2017 [53]. The obtained values of c-di-GMP

were finally normalized per total protein concentrations in the bacteria, measured by Bradford assay (Bio-Rad) at the spectrophotometer at 595 nm wavelength.

2.16. *Caenorhabditis elegans* infection model with PAO1

To test the *in-vivo* potential of PL-18, a nematode infection model was used. The Bristol N2 wild-type *C. elegans* obtained from Caenorhabditis Genetics Center (CGC), University of Minnesota (USA) were maintained at 20 °C on NGM plates seeded with the *Escherichia coli* OP50-1 strain. For the infection assay [54–56], PAO1 was grown overnight at 37 °C with shaking at 180 RPM. The next day, the overnight grown culture was diluted to OD₆₆₀ 1, from which a fresh culture was started with the dilution of 1:100 and grown for ~ 2–3 h at 37 °C until it reached OD₆₆₀ 0.5 (~1 × 10⁸). The bacterial culture was centrifuged to remove the LB media, and the bacterial pellet was resuspended in M9 buffer containing 100 mM Tris-HCl, pH 7.4, 17 mM NaCl. 1 mL of resuspended PAO1 culture was added to each well of the 24-well plates. Along with PAO1, PL-18 (160 μM) or an equal volume of DMSO was added to the experiment and control wells, respectively. 30 young adult animals were transferred to each well and incubated at 25 °C. Worms were scored for viability using a Leica M80 Stereo microscope after 24 h. Worms were classified as dead if they did not exhibit spontaneous movement and failed to respond perceptibly to touch when probed with a wire worm pick.

2.17. Statistical analysis

All statistical analyses were carried out using GraphPad Prism version 8.0.1 for Windows (GraphPad Software, San Diego, California USA, www.graphpad.com). The specific tests recommended by the software are indicated under the relevant Figs.

3. Results

3.1. The screening of PL derivatives for QSI activity

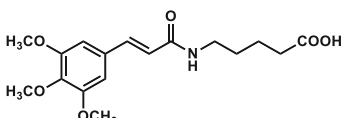
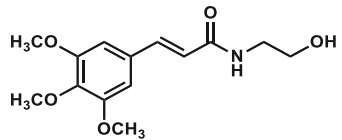
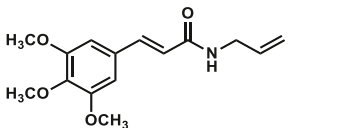
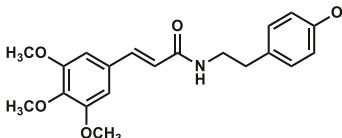
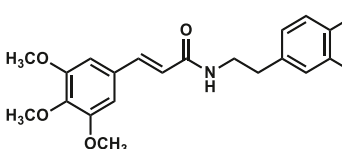
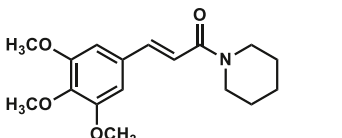
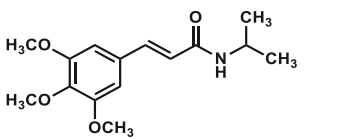
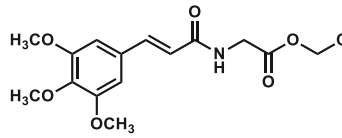
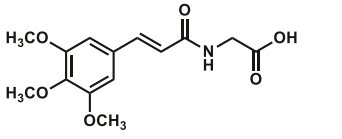
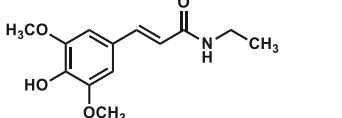
In order to screen Piperlongumine (PL) and 16 of its derivatives for QSI molecules, two reporter bacteria were used *A. tumefaciens* (KYC55) and *C. violaceum* (CV026), which in response to an active QS system produced purple pigment and metabolized X-gal, respectively (representative image of the experiment- [Supplementary Fig. 1](#)). Derivatives were categorized semi-quantitatively into none, low, and high inhibitory activity based on their effect on the color of the cultures in the presence of the Auto-Inducer (AI). PL-18 was found to be the compound with most QSI activity, followed by PL-20 and PL-25. PL-07, PL-17, PL-31, AE-04, and AE-77 which showed low activity. PL and most of the AE series were inactive ([Table 1](#)). Additionally, during the screening process, the antibiotic effect of the derivatives was assessed using disc diffusion tests against *P. aeruginosa*, *E. coli*, *S. aureus*, and *B. subtilis*. None of the compounds were found to have an antibiotic effect (data not shown) except for PL-25 which had a minor antibiotic effect against

Table 1
The screening of piperlongumine derivatives for QSI activity.

No.	Derivative	Molecular Size gr/mol	Chemical Structure	CV026 QSI ^a	KYC55 QSI ^a
1	PL	317.34		-	-
2	PL-07	303.31		-	+
3	PL-17	265.3		+	-
4	PL-18	289.28		++	++
5	PL-20	327.37		-	++
6	PL-25	275.26		++	+
7	PL-31	319.35		-	+

(continued on next page)

Table 1 (continued)

No.	Derivative	Molecular Size gr/mol	Chemical Structure	CV026 QSI ^a	KYC55 QSI ^a
8	PL-23B	337.37		-	-
9	AE-02	281.3		-	-
10	AE-04	277.32		-	+
11	AE-11	357.4		-	-
12	AE-17	373.4		-	-
13	AE-45	305.37		-	-
14	AE-68	279.33		-	-
15	AE-73	323.34		-	-
16	AE-77	295.29		-	+
17	AE-10	251.28		-	-

^a Evaluation of QSI activity of PL derivatives was performed using two reporter bacteria *Chromobacterium violaceum* (CV026) and *Agrobacterium tumefaciens* (KYC55). The derivatives were dried on a thin-layer chromatography (TLC) plate at 40 mM in 20 μ L acetonitrile. Then the bacteria were mixed with an auto-inducer in soft agar layered on top of the TLC and grew overnight. Experiments were repeated three times and relative semi-quantitative results of inhibitory activity were determined as (-) inactive, (+) low activity, (++) high QSI activity.

S. aureus.

3.2. PL-18 QSI activity against *P. aeruginosa*

Since PL-18 showed the highest QSI activity, it was the only derivative that was further evaluated against the clinically relevant *P. aeruginosa* [57]. PL-18 is the di-hydroxy derivative of PL (Table 1, No. 4) [23], and it was found to inhibit three major *P. aeruginosa* QS systems in a dose-dependent manner. Using luminescence reporter bacteria, the luminescence intensity corresponded to the receptor activity (LasR, RhlR, or PqsR). These reporter bacteria cannot synthesize endogenous AI, therefore it was added exogenously. The control group that contained AI and solvent (DMSO) represented 100 % receptor activity. Full kinetic measurements are presented in the Supplementary Fig. 2. PL-18 best inhibits RhlR by 85.6 % at 160 μM with IC_{50} of 18 μM . LasR was inhibited by 76.85 % at 160 μM with a similar IC_{50} value of 22 μM and PqsR was inhibited by 41.3 % at 160 μM with IC_{50} of 181.2 μM (Fig. 1 a, b, and c). The interaction of AI 3-oxo-C12-HSL with the LasR-Ligand Binding Domain (LBD) enables its solubility and its detection in the soluble fraction of the bacterial lysate. It has been reported that the addition of inhibitors that interfere with LasR-LBD reduces the protein's solubility [41]. Upon incubation with PL-18 the solubility of LasR-LBD did not change (Supplementary Fig. 3).

3.3. PL-18 decreases the virulence of *P. aeruginosa*

To determine whether PL-18 affects virulence factors secreted by *P. aeruginosa*, the relative abundance of pyocyanin and rhamnolipids in the bacterial cell-free culture medium was estimated by spectrometry. PL-18 inhibits in a dose-dependent manner these virulence factors (Fig. 2 a and b). PL-18 does not inhibit the swarming motility of

P. aeruginosa, nor the secretion of the protein virulence factor elastase (Supplementary Fig. 4 a and b). Iron is an essential factor for *P. aeruginosa* pathogenicity [58]. PL-18 significantly reduced iron content by 28.6 % in *P. aeruginosa* (PAO1) pellets (Fig. 2 c).

3.4. PL-18 does not affect *P. aeruginosa* growth and viability

To confirm that the QSI and anti-virulence activities of PL-18 are not caused by an antibacterial effect, PL-18 toxicity toward *P. aeruginosa* was determined. Viability was tested by scoring CFUs of PL-18 treated cultures. Bacterial growth was determined by kinetic turbidity measurements. PL-18 found to be not toxic and does not affect *P. aeruginosa* growth at the concentrations tested (see Supplementary Fig. 5 a, and b).

3.5. PL-18 reduces biomass of *P. aeruginosa* biofilm

Since PL-18 inhibits QS, it also implies that it may inhibit biofilm formation. To this end, the anti-biofilm activity of PL-18 was investigated in three different flow conditions set-ups. First, the biofilm was grown for 72 h in the presence of PL-18. Biofilm formation was effectively inhibited by 81 %, at 40 μM (Fig. 3 a, and b). Secondly, PL-18 was dissolved in chloroform and dried on the inner surface of small segments of silicone tubes, then *P. aeruginosa* was introduced and grew as a biofilm for 72 h. Biofilm volume was reduced by 60 % as compared to chloroform treated tubes (Fig. 3 c, and d). When PL-18 was applied on 24 h old biofilm for an additional 24 h biofilm biovolume was 45 % lower than the control (Fig. 3 e, and f). Scanning Electron Microscope (SEM) images of PL-18 coated tubes showed that PL-18 forms crystals that vary in size and shape and are scattered randomly. To assess the morphological properties of PL-18 coated tubes, Scanning Electron Microscopy (SEM) was used to obtain high resolution images of tubes that were untreated,

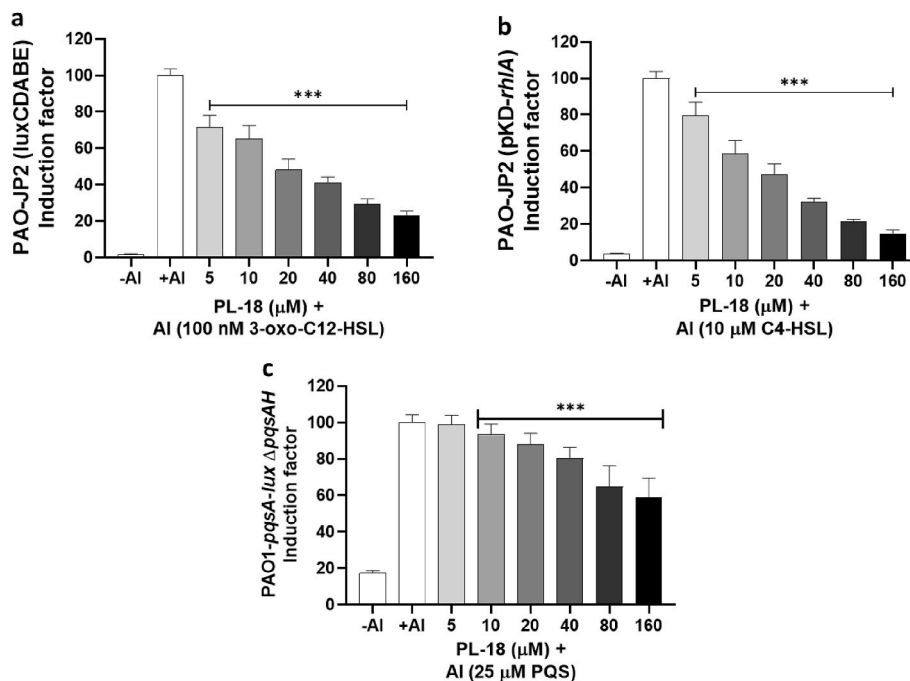


Fig. 1. PL-18 inhibits *P. aeruginosa* QS. QS activity was determined by the bio-reporter bacteria PAO-JP2 harbored a plasmid pKD201 with a lasI promoter coupled to the luxCDABE operon and PAO-JP2 (pKD-rhIA). Both bioreporter bacteria are PAO-JP2 which is a lasI-rhlI double mutant of PAO1. The reporter bacteria were incubated with the appropriate Auto-Inducer (AI) and different PL-18 concentrations for 10 h for kinetic bioluminescence measurement every 15 min. +AI is the control group containing DMSO and the matched AI. (a) PL-18 inhibits LasR activity in the presence of the AI 3-oxo-C12-HSL. (b) PL-18 inhibits RhlR activity in the presence of the AI C4-HSL. (c) PL-18 inhibits PqsR QS activity in the presence of the AI PQS in the bacteria PAO1-pqsA-lux Δ pqsAH. Luminescence was monitored every 15 min for 15 h. For a, b, and c the calculation of the Induction Factor (IF) was: The maximum RLU of each test group was normalized to the maximum RLU of the control group and multiplied by 100 for percentage. Mean \pm SD N = 12 in three independent experiments. One-way ANOVA comparisons of the treatment groups to the control group were followed by Dunnett's multiple comparisons test. 95 % confidence interval (p-values $***\leq 0.0002$).

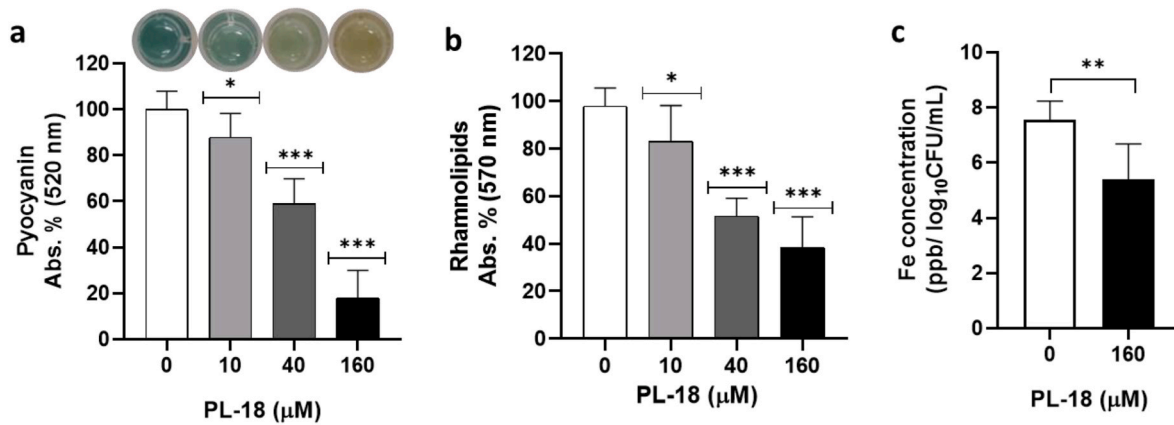


Fig. 2. PL-18 inhibits virulence factors and iron uptake in *P. aeruginosa*. PL-18 was incubated with *P. aeruginosa* for 24 h in LB, then the cultures were centrifuged, and the supernatant was filtered through 0.22 μm . (a) Pyocyanin was extracted using the chloroform-HCl method. Then read at 520 nm in a plate-reader. Representative images of pyocyanin in *P. aeruginosa* cultures are shown in the respective bar. (b) Rhamnolipids quantifications were determined by adjustment of the supernatant to pH 2 and red the absorption at 570 nm. All results were normalized to the control group- (0) containing DMSO. Bars represent mean + SD, N = 9 in three independent experiments. One-way ANOVA comparisons of the treatment groups to the control was followed by Dunnett's multiple comparisons test. 95 % confidence interval (p-values ≤ 0.0332 , ≤ 0.0021 , ≤ 0.0002). (c) The effect of PL-18 on iron uptake was tested ICP-EOS. PAO1 cultures were incubated with PL-18 160 μM for 7 h. Iron content was quantified at 239 nm. The bars represent the iron content in the pellet after the reduction of iron content in the blank and normalized to \log_{10} CFU/mL, mean + SD, N = 6 in triplicates of two independent experiments. The unpaired, two-tailed T-test was used with a 95 % confidence interval, **p-value = 0.0043. (For interpretation of the references to color in this figure legend, the reader is referred to the Web version of this article.)

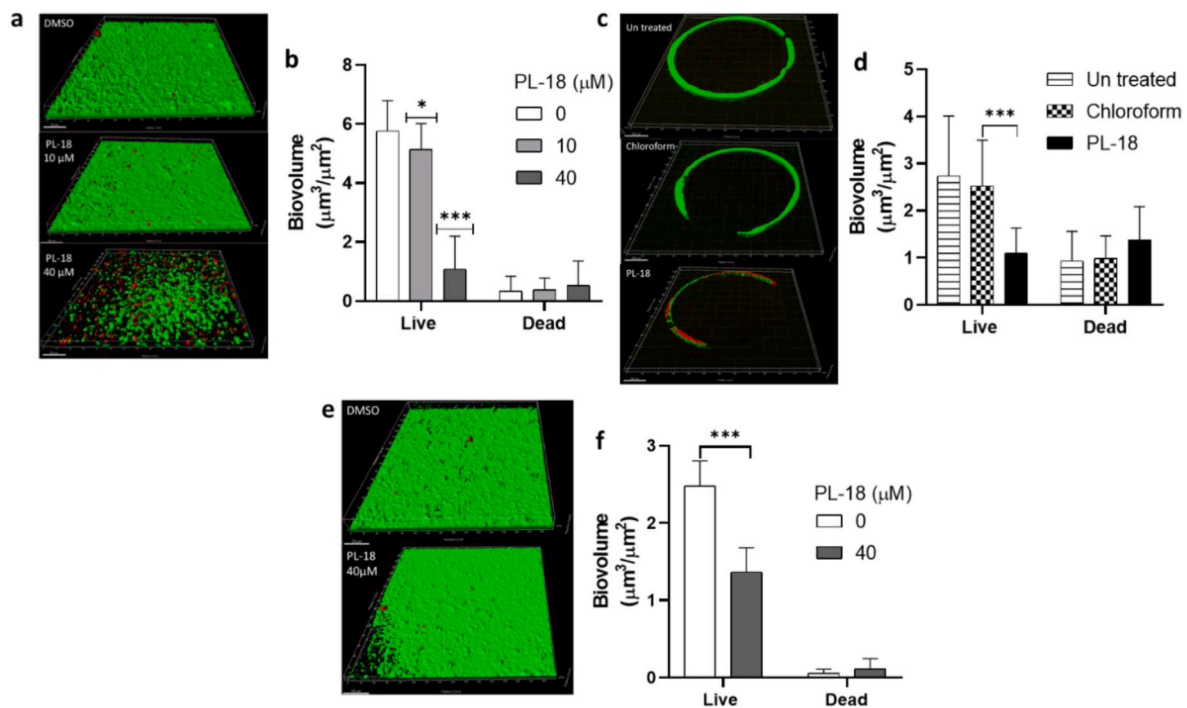


Fig. 3. PL-18 inhibits *P. aeruginosa* biofilm biovolume. PAO1 biofilm was grown in flow conditions. At the end of each experiment, the biofilm was stained using the fluorescent live and dead kit, two channels were detected, SYTO 9 (green) for live cells, and Propidium Iodide (red) for dead cells. The quantification of biovolume was performed in the IMARIS software and normalized to the image area. (a) *P. aeruginosa* biofilm was grown in μ -slide channels (ibidi) in the presence of DMSO (0) or PL-18 at 10 or 40 μM for 72 h. Representative merge images from the CLSM are shown. Scale bar is 50 μm (b) Quantification of fluorescence in a: Live and dead cells were quantified in the presence or absence of PL-18. Bars represent the mean + SD of at least 3 images in each of the duplicates (0) N = 20, (10) N = 21, (40) N = 19, in three independent experiments. (c) Representative images from the CLSM are presented. *P. aeruginosa* was grown as biofilm inside the silicone tubes for 72 h. The biofilm was imaged at 10 \times magnification, and 80 Z plains (each Z plain is 0.5 μm). The scale bar is 200 μm . (d) Quantification of fluorescence in c: Live and dead cells were quantified in the presence or absence of PL-18. Bars represent mean + SD of N = 19 in two independent experiments, in duplicates, at least 5 slices per duplicate were imaged. (e) *P. aeruginosa* biofilm was grown in μ -slide channels (ibidi) for 24 h after DMSO (0) or PL-18 at 40 μM was added to the growth medium for an additional 24 h of growth. Representative merge images from the CLSM are shown. Scale bar is 50 μm (f) Quantification of fluorescence in a: Live and dead cells were quantified in the presence or absence of PL-18. Bars represent mean + SD of 5 images in each of the duplicates, N = 20, in two independent experiments. The statistics for the experiments were: Two-way ANOVA followed by (b) Dunnett's and (d, f) Tukey's multiple comparisons test. 95 % confidence interval (p-values ≤ 0.0002). (For interpretation of the references to color in this figure legend, the reader is referred to the Web version of this article.)

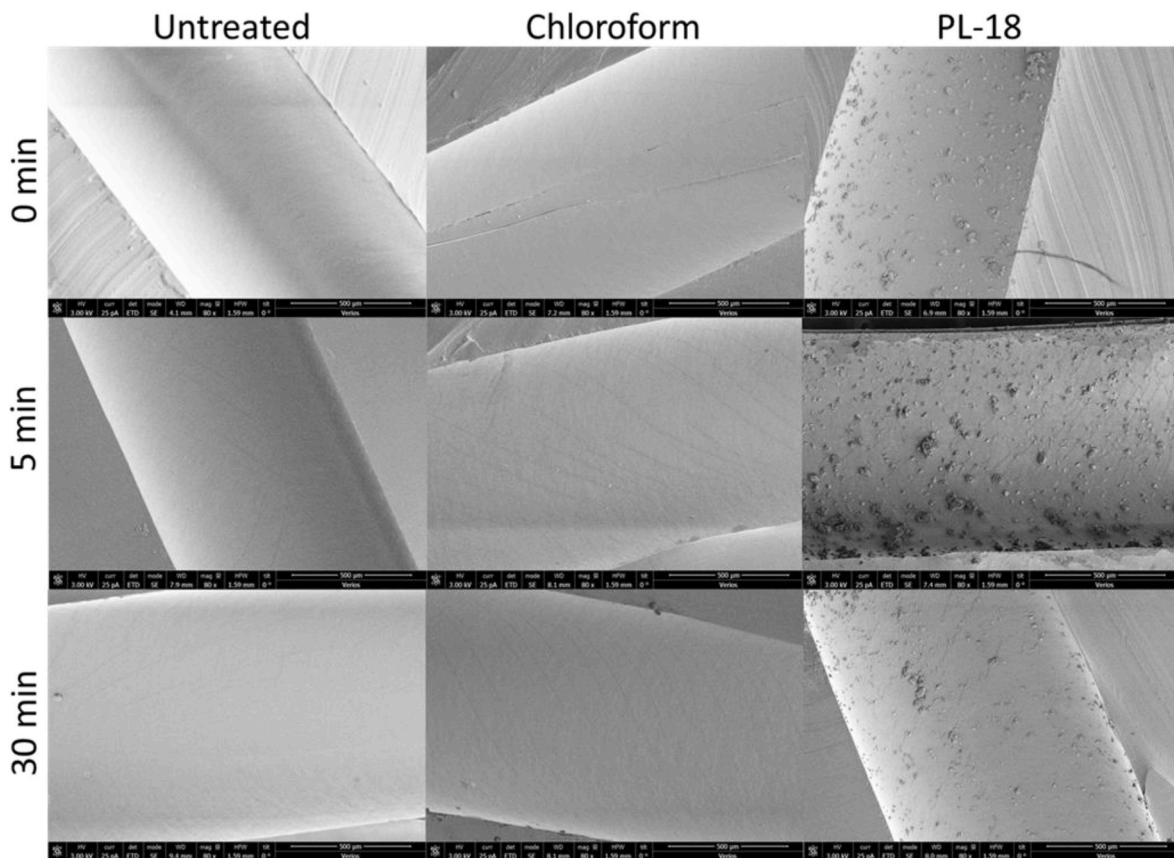


Fig. 4. The presence of PL-18 crystals on coated silicone tubes: SEM micrographs of silicon tubes; untreated, chloroform treated, or PL-18 treated tubes, after drying (0 min), after 5 min and after 30 min of AB medium flow (3 mL/h). Scale bar 500 μm .

chloroform treated, or PL-18 treated. Importantly, the crystals are not washed out following the flow of growth media for 30 min at Room Temperature (RT) (Fig. 4).

3.6. PL-18 effect on *P. aeruginosa* transcriptome, including sulfur and iron metabolism pathways

To study the PL-18 mode of action, an unbiased transcriptome analysis approach was undertaken. The peak QS activity of *P. aeruginosa* reporter bacteria is after incubation for 7 h. Supplementary Fig. 2 a and b). PL-18 (160 μM) or DMSO was added for 7 h then RNA was extracted and quantified. A total of 5568 genes were expressed, and 1096 (19.5%) genes were significantly up or down regulated. The list of all significant genes is in Supplementary Table 1 sheet 1. The heat map shows the differences in gene expression between the control and PL-18 treated cultures following a cut off of two-fold of Change (FC). 116 genes were up regulated (2.08%) and 137 genes were down regulated (2.46%) by PL-18, altogether 253 genes (Fig. 5 a). A volcano plot showed that statistically, the transcriptome analysis is valid (Supplementary Fig. 6). To further validate the transcriptome results, RT-qPCR was performed. The expression of several genes was tested, including QS related genes (Fig. 5 b). The RT-qPCR experiments, confirm the transcriptome results.

STRING protein network analysis [59] was applied to the 253 genes. The genes were uploaded to the Cytoscape software [60] and STRING database. The analysis resulted in a total of 246 nodes, single-stones were removed from the network, and 1249 edges and PPI (protein-protein interaction) were detected with an enrichment p-value lower than $1e-16$ (Fig. 6). The network includes nine clusters, as expected, and confirmed, the QS cluster was down regulated, including the *pqs* operon, anthranilate synthesis, *rhlI*, and *vqsR* (Fig. 6 cluster 2).

Two large clusters were identified, one related to iron metabolism which is down regulated (Fig. 6 cluster 4), and the other related to sulfur metabolism which is mostly up regulated (cluster 1, Supplementary Fig. 7). Of the 137 genes that were down regulated, 66 genes (48%) are related to iron metabolism including the *nir* operon cluster that is repressed by PL-18 (cluster 3) which is related to heme D1 biosynthesis. The genes that are associated with iron uptake, heme production and uptake, iron scavenging, siderophore synthesis, iron regulation, storage, and homeostasis are listed in Supplementary Table 1 Excel sheet 2. In addition, upon incubation with PL-18 several genes that are related to biofilm formation were reduced as well (Supplementary Fig. 8), including genes related to c-di-GMP, and *psl* polysaccharide production. Cyclic-di-GMP is a secondary messenger employed by bacteria and is associated with biofilm formation [61]. Thus, the c-di-GMP levels were measured in *P. aeruginosa* cultures exposed to PL-18 at 40 and 160 μM or DMSO (control) at the same conditions as in the transcriptome analysis. The PL-18 treated samples showed lower c-di-GMP concentrations than the control samples, but due to variation in the data set, the results were not statistically significant as tested by One-way ANOVA (Supplementary Fig. 9).

As shown above, PL-18 strongly reduced iron acquisition and homeostasis (Figs. 2 c and Fig. 6). The experiments presented above (Figs. 1, 2, 5 and 6) were all conducted at sufficient iron concentrations (LB medium). Therefore, the effect of PL-18 QSI activity at low iron conditions was studied in order to determine whether PL-18 activity depends on iron concentration. Using the reporter luminescence bacteria- PAO-JP2 to measure LasR and RhIR QS activity an iron chelator ethylenediamine-N,N'-bis(2-hydroxyphenylacetic acid) (EDDHA) was added to reduce iron concentration. As shown in Supplementary Fig. 10, the addition of EDDHA without the AI did not result in QS activation in

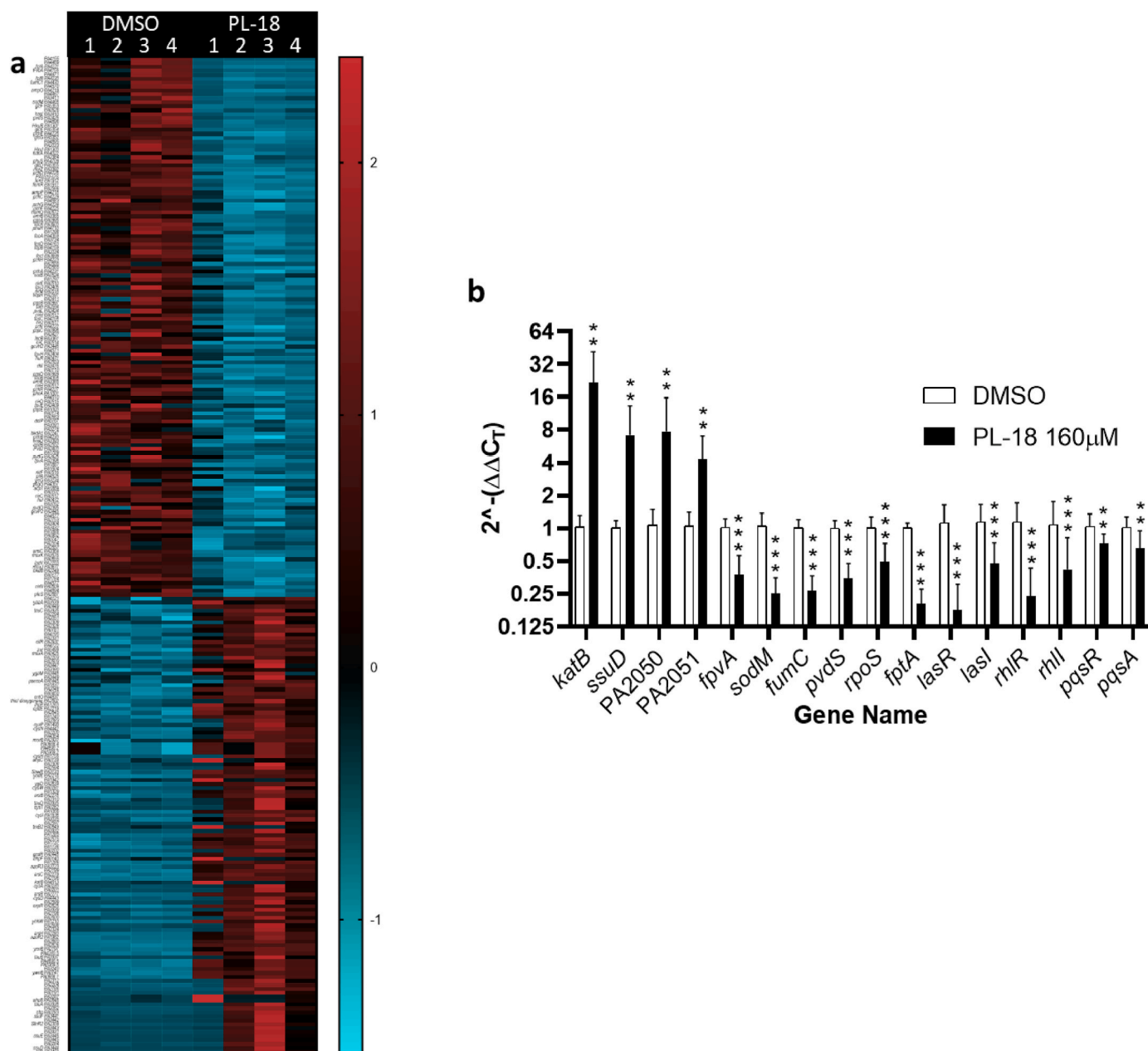


Fig. 5. PL-18 alters gene expression of *P. aeruginosa*. *P. aeruginosa* was incubated with 160 μ M PL-18 for 7 h, followed by RNA extraction and cDNA synthesis. Subsequently, next-generation sequencing and quantification of gene expression was performed. (a) Heat-map of genes that are beyond the cutoff of 2 Fold of Change (FC) is presented. Left column-four replicates of control DMSO treated cultures. Right column-four replicates of PL-18 treated cultures. Downregulated genes are cyan and red are upregulated genes. (b) Validation of several genes including QS related genes by RT-qPCR. Target genes were amplified by RT-qPCR. For pqsR, fpvA, and fumC N = 11, all the other N = 12, Mean + SD, in two independent experiments with 3 biological replicates and 2 technical replicates. For comparison, a two-tailed *t*-test between DMSO and PL-18 samples of each of the primers was performed, with a 95 % confidence interval (p-values $^* \leq 0.0332$, $^{**} \leq 0.0021$, $^{***} \leq 0.0002$). (For interpretation of the references to color in this figure legend, the reader is referred to the Web version of this article.)

both reporter bacteria. However, in the presence of AI and EDDHA a dose dependent increase in QS activity of mainly RhlR was observed. In the presence of PL-18, its QSI activity was not affected by EDDHA concentrations, thus, PL-18 activity is independent of iron concentrations.

3.7. PL-18 reduces the death of *C. elegans* infected with PAO1

To test the in-vivo effect of PL-18, *C. elegans* nematodes were infected with PAO1 and treated simultaneously with PL-18 or vehicle. Dead nematodes were scored after 24 Hrs. The results in Fig. 7 show that PL-18 treated nematodes were significantly protected. 43.3 % of control

nematodes were dead as opposed to only 24.6 % of PL-18 treated nematodes.

4. Discussion

In this study, PL and 16 of its derivatives were screened to identify QSI molecules for their therapeutic potential benefits in treating resistant bacterial infections. PL was tested against QS of *Chromobacterium violaceum* (CV026) and *Agrobacterium tumefaciens* (KYC55) and was found to be inactive. In contrast to PL, PL-18 showed potent QSI activity in four different Gram-negative bacterial HSL systems, corresponding to four different receptors and AI molecules: CviR-3-oxo-C6-HSL from

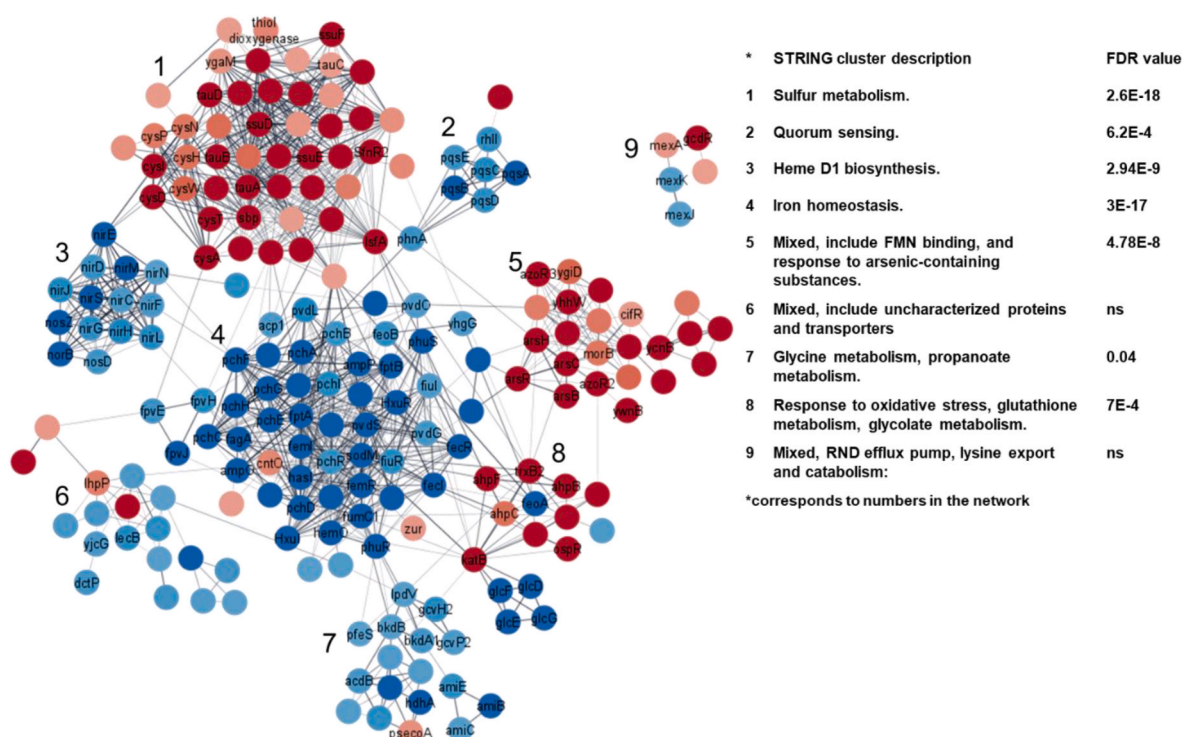


Fig. 6. Transcription enrichment and clustering. The full STRING protein-protein interaction network database on the Cytoscape software was used. All genes beyond the cut off of 2 FC were analyzed with a confidence score default of 0.4. The red circles are upregulated and the blue circles are downregulated genes. The color intensity corresponds to the level of the FC. The thickness of the strings emphasizes the confidence of the interaction. A list of the different clusters and their statistical value (FDR) is shown. FMN- Flavin mononucleotide, RND- Resistance-Nodulation-Division. (For interpretation of the references to color in this figure legend, the reader is referred to the Web version of this article.)

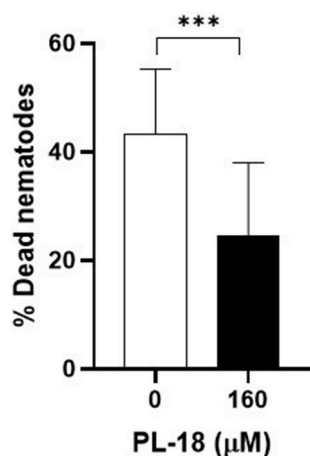


Fig. 7. PL-18 reduces nematodes death in PAO1 infection model. *C. elegans* were exposed to PAO1 with PL-18 at 160 μM or with DMSO and percentage of dead animals was plotted after 24 h. Mean + SD N = 15, of triplicates in five independent experiments, each biological replica is including 30 worms. The p-value equals 0.0004 as determined by the un-paired, two-tailed *t*-test.

CV026, TraR-3-oxo-C8-HSL from KYC55, and two *P. aeruginosa* receptors LasR-3-oxo-C12-HSL, and RhlR-C4-HSL. These receptors are homologous proteins in the LuxR family. They respond to different AIs that differ in the carbon chain length, saturation, and substitution on the third carbon (oxo or hydroxyl). The degree of specificity of the receptors varies and depends on the above chemical parameters [62]. When inhibition of QS was tested, it was observed that when the methoxy groups of PL were substituted by hydroxy groups, QS was inhibited. This substitution correlates with better QSI activity: PL-18 > PL-25 > PL-20 >

PL-07, PL-17, PL-31, AE-04, AE-77. PL was inactive as well as the rest of the AE series tested. To understand the importance of the 5,6-dihydropyridin-2-one ring of PL, it was replaced with different amines as in PL-17, PL-20, PL-31, and in all the AE series, only a minor improvement in QSI activity was observed in comparison with PL, which is inactive. Earlier reports suggest that C2-C3 olefin in 5,6-dihydropyridin-2-one ring of PL is crucial for ROS generation [26,29]. PL is a ROS generator; however, replacing methoxy groups with hydroxy groups (i.e., PL-18) enables their antioxidant activity [23,63]. Although minor, the improved QSI activity of PL-17, PL-20, and PL-31 which lack the 5, 6-dihydropyridin-2-one ring, suggests that ROS generation may not be relevant for QSI activity. To further understand the contribution of the alkaloid ring, new variants of the molecule will be synthesized where the two hydroxy moieties in the aromatic ring will remain constant (QS active) and the alkaloid ring will vary.

Of the tested compounds PL-18 was the most QSI active and therefore was selected for further study. PL-18 non-selectively inhibited several HSL receptors, which can be explained either by its interaction with a conserved receptor structure or by affecting a common QS-modulating signaling pathway. Since the addition of PL-18 did not affect the solubility of LasR-LBD (Supplementary Fig. 3), it is possible that it does not interact directly with it. AI production can be a target for QSI activity. The QSI activity of PL-18 through AI synthesis cannot be determined using the five reporter strains of KYC55, CV026, *P. aeruginosa* (PAO-J2), and PAO1 CTX-luxpqsA Δ pqsAH, since they are null mutants of the AI synthetase, therefore lacking AI endogenous production. Nevertheless, the expression of the three AI synthetase genes (*lasI*, *rhlI*, and *pqsAH*) was down regulated by PL-18 as shown in the transcriptome analysis and the RT-qPCR validation experiments. The QS receptors complexed with their AIs, act as transcription factors, which autologously activate their own gene expression including the *lasI*, *rhlI*, and *pqsAH* synthetase genes and the receptor coding genes *lasR*, *rhlR*, and *pqsR* [64]. These results suggest the possibility that PL-18

may modulate the synthesis of AI via a reduction of the synthetase gene expression.

It is known that when QS is inhibited, the virulent behavior of *P. aeruginosa* is inhibited as well [65]. Indeed, PL-18 effectively reduced rhamnolipids, and pyocyanin content in the cell-free supernatant, as well as intracellular iron concentration and reduction in biofilm biovolume. Nevertheless, the transcription level of rhamnolipids and pyocyanin synthesis related genes (i.e., *rhlAB*, and *phz* operon) was not changed in the transcriptome analysis, therefore suggesting that PL-18 affects rhamnolipids and pyocyanin levels post-transcriptionally. PL-18 does not inhibit other virulence features such as motility and elastase secretion. This can be explained by the existence of alternative regulatory pathways not inhibited by PL-18 [12,66]. These findings suggest that PL-18 affects multiple targets that directly or indirectly inhibit QS systems.

Biofilms are complex, their formation and dispersal are regulated and balanced in response to outside stimuli such as QS, and different types of stress. PL-18 effectively decreases the formation of *P. aeruginosa* biofilm under flow conditions both on glass and silicon surfaces (81 % and 60 %, respectively). PL-18 crystals are stable on the surface of the silicon tubes and remain there even after washing. Furthermore, PL-18 decreases the biomass of a 24 h old biofilm by 45 %. These results are significant for the further development of treated medical implants and catheters.

The transcriptome analysis revealed that PL-18 reduced biofilm biomass by affecting several biofilm related features. Multiple factors influence the balance between the biofilm and planktonic lifestyles. Among these factors are levels of c-di-GMP, a secondary signaling metabolite that is responsible for the gene expression of many genes that are related to motility, biofilm development, and virulence. The intracellular concentration of c-di-GMP is coordinated by multiple genes such as *rpoS* and *tpbB*. *rpoS* is a regulator responsible for the elevation of the c-di-GMP levels, resulting in increased biofilm formation [67,68]. It has also been shown that *rpoS* regulates QS in *P. aeruginosa* [69]. The gene *tpbB* (*yfiN*, PA1120) codes for di-guanylate cyclase and is positively regulated by LasR [70]. Both genes were down regulated by PL-18, which means that PL-18 may modulate c-di-GMP levels. When c-di-GMP levels were measured, they were reduced in the PL-18 treated groups, but the differences were not statistically significant. These results suggest that although c-di-GMP may still have a role in the reduction of biofilm biomass, PL-18 may additionally target other systems.

An important characteristic of the biofilm architecture is the Extracellular Matrix (ECM), which is a complex mixture of molecules, such as polysaccharides, eDNA, and proteins that establishes the biofilm structure and stability. QS regulates the production and secretion of several ECM components such as pyocyanin, siderophores, eDNA, and rhamnolipids [71]. Inhibition of QS results in the inhibition of biofilm formation [72]. Likewise, biofilm biomass was reduced by PL-18. In *P. aeruginosa* *psl*, *pel*, and *alg* are the three main operons that are responsible for the production of the polymeric substances of the ECM [73]. The ECM is crucial for *P. aeruginosa* survival in biofilm and inside hosts and their production is partially controlled by QS [70,71,74–76]. The following genes are all down regulated by PL-18: *pslACDEFG* and *algZ* (*amrZ*); The fructose or mannose-binding protein coded by *lecB* which is also important for biofilm stability [71]; *fumC1*, and *sodM* (also called *sodA*) coding for fumarate hydratase and superoxide dismutase respectively are correlated with the overproduction of alginate [77,78]. Altogether, these results are consistent with the reduction of biofilm biomass by PL-18. Thus, the experimental results and the transcriptional analysis show that *P. aeruginosa* biofilm formation is impaired due to QS inhibition, and attenuation of transcription of ECM components (e.g., *lecB* and *psl* operon).

Iron is essential for many aspects of *P. aeruginosa* life, as well as for biofilm formation. Nevertheless, it can be toxic, therefore, iron acquisition is tightly regulated [79]. Iron within the host is a limiting factor

for *P. aeruginosa* infections. Iron uptake systems are up regulated, especially during infection to scavenge iron from the host. Maintaining external low iron concentration is one way the host restricts the infection progression, therefore, the iron systems of *P. aeruginosa* are proposed to be targets for infection attenuation [80]. When PL-18 was incubated with *P. aeruginosa* cultures, many iron-related genes were repressed and less iron was acquired by the bacteria in comparison to the control. These results are in contrast to the effect of chelators on iron related gene expression. If iron would be chelated and its concentration reduced, QS and iron starvation related genes would be expected to increase and not to decrease, as shown here for the QS receptor *RhlR*, and *RhlAB* and *RhlI* as shown by others [58,81]. In addition, the production of the AI of the *pqs* system, PQS, is increased by low iron concentration. PQS has chelator activity and is a positive regulator of iron acquisition [82,83]. The expression of the QS related genes *pqsABCDE* operon, and *pqsH* which are regulated by *RhlR* and *PqsR*, were down regulated by PL-18. Their down regulation may explain the inhibition in iron uptake and homeostasis related genes. Other iron related regulatory genes were modulated by PL-18. Two genes that are up regulated are PA2051 codes for Fe^{2+} di-citrate sensor, membrane protein and its conjugated RNA polymerase sigma factor PA2050 [84]. PA2384 positively regulates PA2050 [85]. Interestingly, the location of PA2051 within the STRING network is central and is connected to *pvdS* and *tauA* which in turn, each one of them is connected to the majority of genes in the iron and sulfur metabolism clusters. *pvdS* [86] and PA2384 [87] are important iron starvation response regulators that are down regulated by PL-18, therefore, their down regulation may have a role in the inhibition of iron uptake. The *sigX* (PA1776) gene belongs to the Extra Cytoplasmatic Function (ECF) receptors family. Bacteria harboring this mutant gene have reduced virulence and biofilm formation [88] and was repressed by PL-18. PA2051, and *pvdS* also belong to the ECF family [84]. In summary, low iron concentrations detected in the bacteria following incubation with PL-18 show that PL-18 reduces iron concentration by down and up regulation of iron uptake related genes and not by iron chelation.

Sulfur metabolism related genes are also highlighted by the PL-18 modulated transcriptome. In contrast to iron metabolism genes that are mainly down regulated, sulfur metabolism genes were shown to be mostly up regulated. As mentioned above, the PA2051 gene connects between iron and sulfur metabolism genes in opposite directions. It will be of interest to investigate the PA2051 functions. As an example of the significance of sulfur metabolism genes up regulation, hydrogen sulfide (H_2S) was found to enhance LasR activity [89]. Since, PL-18 up regulates sulfur metabolism genes related to the reduction and bio-incorporation of sulfur, including possible decrease of H_2S , resulting in the neutralization of its enhancement of LasR activity. Furthermore, sulfur compounds enable antibiotic resistance of *P. aeruginosa*. H_2S produced by the bacteria activates the *mexAB* operon that codes for Resistance-Nodulation-Cell Division (RND) antibiotics multidrug efflux transporter genes in response to oxidative stress induced by antibiotics [90]. In the present study, these two genes (*mexAB*) were up regulated, therefore, possibly enabling antibiotic resistance. Other RND genes were unchanged except for *MexJK* that were down regulated. The up regulation of sulfur metabolism related genes influences multiple processes including QS and antibiotic resistance. The association between iron and sulfur systems, QS, biofilm formation, and antibiotic resistance which is not fully understood and needs further research can make use of reagents such as PL-18 to study these complex interactions.

PL-18 was previously shown not to be cytotoxic to several cell-lines and to have antioxidant properties [23]. Similarly, PL-18 appears not to inhibit *P. aeruginosa* growth and viability, hence, the inhibitory activities reported here were not due to toxic antibiotic activity. Moreover, PL-18 protects *P. aeruginosa* infected *C. elegans in-vivo*. Therefore we conclude that PL-18 has the potential to be further developed as an inhibitor of *P. aeruginosa* biofilm formation and virulence, with the advantage of reduced selection of antibiotic resistant strains.

CRedit authorship contribution statement

Yael Schlichter Kadosh: Writing – original draft, Visualization, Validation, Methodology, Investigation, Formal analysis, Conceptualization. **Subramani Muthuraman:** Writing – review & editing, Methodology, Investigation, Formal analysis, Conceptualization. **Khairun Nisaa:** Conceptualization, Methodology, Validation, Writing – review & editing. **Anat Ben-Zvi:** Conceptualization, Resources, Supervision, Writing – review & editing. **Danit Lisa Karsagi Byron:** Conceptualization, Methodology, Writing – review & editing. **Marilou Shagan:** Conceptualization, Methodology, Writing – review & editing. **Alexander Brandis:** Conceptualization, Formal analysis, Validation, Writing – review & editing. **Tevie Mehlman:** Conceptualization, Formal analysis, Methodology, Validation, Writing – review & editing. **Jacob Gopas:** Writing – original draft, Visualization, Supervision, Resources, Funding acquisition, Conceptualization. **Rajendran Saravana Kumar:** Writing – review & editing, Visualization, Validation, Supervision, Resources, Formal analysis, Conceptualization. **Ariel Kushmaro:** Writing – review & editing, Visualization, Validation, Supervision, Resources, Funding acquisition, Conceptualization.

Declaration of competing interest

The authors declare no competing interests.

Data availability

Data will be made available on request.

Acknowledgments

Y.S.K thanks her Ph.D. fellowship from the Israel Ministry of Science & Technology. Furthermore, the authors thank the Avram and Stella Goldstein-Goren fund for partial support. We thank Esti Kramarsky-Winter for her scientific comments and editing. For technical assistance, several persons are acknowledged from The Ilse Katz Centre for Nanoscale Science, Ben-Gurion University of the Negev, Israel: CLSM imaging Dr. Alon Zilha (also from the Technology center NIBN, BGU), SEM imaging with the help of Dr. Roxana Golan, ICP-EOS was performed by Dr. Bar Elisha, and Dr. Albert Batushansky. The transcriptome sequencing and QA were performed at the Genomics and Microbiome Core Facility (GMCF) at Rush University by Dr. Stefan Green. Bioinformatic analysis was done in the BGU Bioinformatics Core Facility by Dr. Liron Levine. A.K and Y.S.K also thank the Avram and Stella Goldstein-Goren fund for partial support. The bacterial strains (i.e., CV026, PQS, and PAO-JP2) were kindly provided by Prof. Paul Williams from the Centre for Biomolecular Sciences, University of Nottingham, UK, and Prof. Michael M. Meijler from the Department of Chemistry and NIBN, BGU. Additionally, we thank Prof. Ehud Banin from The Mina & Everard Goodman Faculty of Life Sciences at Bar-Ilan University and a member of the Institute of Nanotechnology and Advanced Materials for great scientific advice. Finally, we want to thank Dr. Lana Meshnik for her help with the nematode experiments.

Appendix A. Supplementary data

Supplementary data to this article can be found online at <https://doi.org/10.1016/j.biofilm.2024.100215>.

References

- [1] Habboush Y, Guzman N. Antibiotic resistance. In: *StatPearls*; anonymous. Treasure Island (FL): StatPearls Publishing; 2020.
- [2] MacLean RC, Millan AS. The evolution of antibiotic resistance. *Science* 2019;365:1082–3.
- [3] Morrison KD, Martin KA, Wimpenny JB, Loots GG. Synthetic antibacterial minerals: harnessing a natural geochemical reaction to combat antibiotic resistance. *Sci Rep* 2022;12:1–11.
- [4] Miranda SW, Asfahl KL, Dandekar AA, Greenberg EP. *Pseudomonas aeruginosa* Quorum sensing. *Adv Exp Med Biol* 2022;1386:95–115.
- [5] Liu G, Catacutan DB, Rathod K, Swanson K, Jin W, Mohammed JC, Chiappino-Pepe A, Syed SA, Fraxis M, Rachwalski K, et al. Deep learning-guided discovery of an antibiotic targeting acinetobacter baumannii. *Nat Chem Biol* 2023;19:1342–50.
- [6] Miller MB, Bassler BL. Quorum sensing in bacteria. *Annu Rev Microbiol* 2001;55:165–99.
- [7] Yates EA, Philipp B, Buckley C, Atkinson S, Chhabra SR, Sockett RE, Goldner M, Dessaux Y, Cámara M, Smith H, et al. N-acylhomoserine Lactones undergo lactonolysis in a pH-, temperature-, and acyl chain length-dependent manner during growth of *Yersinia pseudotuberculosis* and *Pseudomonas aeruginosa*. *Infect Immun* 2002;70:5635–46.
- [8] Trautmann M, Lepper PM, Haller M. Ecology of *Pseudomonas aeruginosa* in the intensive care unit and the evolving role of water outlets as a reservoir of the organism. *Am J Infect Control* 2005;33:41.
- [9] Azam MW, Khan AU. Updates on the pathogenicity status of *Pseudomonas aeruginosa*. *Drug Discov Today* 2019;24:350–9.
- [10] Brint JM, Ohman DE. Synthesis of multiple exoproducts in *Pseudomonas aeruginosa* is under the control of RhlR-RhlI, another set of regulators in strain PAO1 with homology to the autoinducer-responsive LuxR-LuxI family. *J Bacteriol* 1995;177:7155–63.
- [11] Passador L, Cook JM, Gambello MJ, Rust L, Iglewski BH. Expression of *Pseudomonas aeruginosa* virulence genes requires cell-to-cell communication. *Science* 1993;260:1127–30.
- [12] Khan F, Pham DTN, Oloketuyi SF, Kim Y. Regulation and controlling the motility properties of *Pseudomonas aeruginosa*. *Appl Microbiol Biotechnol* 2020;104:33–49.
- [13] Mukherjee S, Moustafa D, Smith CD, Goldberg JB, Bassler BL. The RhlR quorum-sensing receptor controls *Pseudomonas aeruginosa* pathogenesis and biofilm development independently of its canonical homoserine lactone autoinducer. *PLoS Pathog* 2017;13.
- [14] O'Loughlin CT, Miller LC, Siryaporn A, Drescher K, Semmelhack MF, Bassler BL. A quorum-sensing inhibitor blocks *Pseudomonas aeruginosa* virulence and biofilm formation. *Proc Natl Acad Sci U S A* 2013;110:17981–6.
- [15] Liu J, Hou J, Chang Y, Peng L, Zhang X, Miao Z, Sun P, Lin J, Chen W. New pqs Quorum sensing system inhibitor as an antibacterial synergist against multidrug-resistant *Pseudomonas aeruginosa*. *J Med Chem* 2022;65:688–709.
- [16] McGrath S, Wade DS, Pesci EC. Dueling Quorum sensing systems in *Pseudomonas aeruginosa* control the production of the *Pseudomonas* quinolone signal (PQS). *FEMS Microbiol Lett* 2004;230:27–34.
- [17] Hall-Stoodley L, Costerton JW, Stoodley P. Bacterial biofilms: from the natural environment to infectious diseases. *Nat Rev Microbiol* 2004;2:95–108.
- [18] Percival SL, Suleman L, Vuotto C, Donelli G. Healthcare-associated infections, medical devices and biofilms: risk, tolerance and control. *J Med Microbiol* 2015;64:323–34.
- [19] Pearson JP, Feldman M, Iglewski BH, Prince A. *Pseudomonas aeruginosa* cell-to-cell signaling is required for virulence in a model of acute pulmonary infection. *Infect Immun* 2000;68:4331–4.
- [20] Cizek-Lenda Marta, Strus Magdalena, Walczewska Maria, Majka Grzegorz, Machul-Zwirbla Agnieszka, Mikołajczyk Diana, Górska Sabina, Gamian Andrzej, Chain Benjamin, Marcinkiewicz Janusz. *Pseudomonas aeruginosa* biofilm is a potent inducer of phagocyte hyperinflammation. *Inflamm Res* 2019;68:397–413.
- [21] Tasneem S, Liu B, Li B, Choudhary MI, Wang W. Molecular pharmacology of inflammation: medicinal plants as anti-inflammatory agents. *Pharmacol Res* 2019;139:126–40.
- [22] Golan-Goldhirsh A, Gopas J. Plant derived inhibitors of NF- κ B. *Phytochemistry Rev* 2014;13:107–21.
- [23] Subramani M, Ramamoorthy G, Hemaiswarya S, Waidha K, Brindha J, Balamurali MM, Doble M, Rajendran S. Hydroxy piperlongumines: synthesis, antioxidant, cytotoxic effect on human cancer cell lines, inhibitory action and ADMET studies. *ChemistrySelect* 2020;5:11778–86.
- [24] Subramani M, Rajendran SK. Mild, metal-free and protection-free transamidation of N-Acyl-2-Piperidones to amino acids, amino alcohols and aliphatic amines and esterification of N-Acyl-2-Piperidones. *Eur J Org Chem* 2019;2019:3677–86.
- [25] Kumar S, Kamboj J, Suman n, Sharma S. Overview for various aspects of the health benefits of piper longum linn. *Fruit. J Acupunct Meridian Stud* 2011;4:134–40.
- [26] Bezerra DP, Pessoa C, de Moraes MO, Saker-Neto N, Silveira ER, Costa-Lotufo LV. Overview of the therapeutic potential of piperlongumine (piperlongumine). *Eur J Pharmaceut Sci* 2013;48:453–63.
- [27] Bezerra DP, Militão GCG, de Castro FO, Pessoa C, de Moraes MO, Silveira ER, Lima MAS, Elmiro FJM, Costa-Lotufo LV. Piperlongumine induces inhibition of leukemia cell proliferation triggering both apoptosis and necrosis pathways. *Toxicol Vitro* 2007;21:1–8.
- [28] Zheng J, Son DJ, Gu SM, Woo JR, Ham YW, Lee HP, Kim WJ, Jung JK, Hong JT. Piperlongumine inhibits lung tumor growth via inhibition of nuclear factor kappa B signaling pathway. *Sci Rep* 2016;6:26357.
- [29] Adams DJ, Dai M, Pellegrino G, Wagner BK, Stern AM, Shamji AF, Schreiber SL. Synthesis, cellular evaluation, and mechanism of action of piperlongumine analogs. *Proc Natl Acad Sci U S A* 2012;109:15115–20.
- [30] Mgebaheurike EE, Stålnacke M, Vuorela H, Holm Y. Antimicrobial and synergistic effects of commercial piperine and piperlongumine in combination with conventional antimicrobials. *Antibiotics* 2019;8.

- [31] Hentzer M, Riedel K, Rasmussen TB, Heydorn A, Andersen JB, Parsek MR, Rice SA, Eberl L, Molin S, Hoiby N, et al. Inhibition of Quorum sensing in *Pseudomonas aeruginosa* biofilm bacteria by a halogenated furanone compound. *Microbiology* 2002;148:87–102.
- [32] Liu Y, Li J, Li H, Deng S, Jia A. Quorum sensing inhibition of hordenine analogs on *Pseudomonas aeruginosa* and *Serratia marcescens*. *Synth Syst Biotechnol* 2021;6:360–8.
- [33] Muthuraman S, Sinha S, Vasavi CS, Waidha KM, Basu B, Munussami P, Balamurali MM, Doble M, Saravana Kumar R. Design, synthesis and identification of novel coumapherine derivatives for inhibition of human 5-LOX: antioxidant, pseudoperoxidase and docking studies. *Bioorg Med Chem* 2019;27:604–19.
- [34] Joëlsson AC, Zhu J. LacZ-based detection of acyl-homoserine lactone quorum-sensing signals. *Current Protocols in Microbiology* 2006;3:1C.2.1–9.
- [35] Zhu Jun, Chai Yunrong, Zhong Zengtao, Li Shunpeng, Winans Stephen C. *Agrobacterium* bioassay strain for ultrasensitive detection of N-acylhomoserine lactone-type quorum-sensing molecules: detection of autoinducers in mesorhizobium huakuii. *Appl Environ Microbiol* 2003;69:6949–53.
- [36] Kadosh Y, Muthuraman S, Yaniv K, Baruch Y, Gopas J, Kushmaro A, Kumar RS. Quorum sensing and NF- κ B inhibition of synthetic coumapherine derivatives from piper nigrum. *Molecules* 2021;26.
- [37] Ganin H, Tang X, Meijler MM. Inhibition of *Pseudomonas aeruginosa* Quorum sensing by AI-2 analogs. *Bioorg Med Chem Lett* 2009;19:3941–4.
- [38] Duan K, Surette MG. Environmental regulation of *Pseudomonas aeruginosa* PAO1 las and rhl quorum-sensing systems. *J Bacteriol* 2007;189:4827–36.
- [39] Brouwer S, Pustelny C, Ritter C, Klünkert B, Narberhaus F, Häussler S. The PqsR and RhlR transcriptional regulators determine the level of *Pseudomonas* quinolone signal synthesis in *Pseudomonas aeruginosa* by producing two different pqsABCDE mRNA isoforms. *J Bacteriol* 2014;196:4163–71.
- [40] Feathers JR, Richael EK, Simanek KA, Fromme JC, Paczkowski JE. Structure of the RhlR-PqsE complex from *Pseudomonas aeruginosa* reveals mechanistic insights into quorum-sensing gene regulation. *Structure* 2022;30:1626–1636.e4.
- [41] Markus V, Golberg K, Teralki K, Ozer N, Kramarsky-Winter E, Marks RS, Kushmaro A. Assessing the molecular targets and mode of action of furanone C-30 on *Pseudomonas aeruginosa* Quorum sensing. *Molecules* 2021;26.
- [42] Sarabhai S, Sharma P, Capalash N. Ellagic acid derivatives from *Terminalia chebula* retz. Downregulate the expression of Quorum sensing genes to attenuate *Pseudomonas aeruginosa* PAO1 virulence. *PLoS One* 2013;8:e53441.
- [43] Malešević M, Lorenzo FD, Filipić B, Stanisavljević N, Novović K, Senerović L, Polović N, Molinaro A, Kojić M, Jovčić B. *Pseudomonas aeruginosa* Quorum sensing inhibition by clinical isolate delftia tsuruhatensis 11304: involvement of N- α -octadecanoylhomoserine Lactones. *Sci Rep* 2019;9:1–13.
- [44] Yehuda N, Gheber LA, Kushmaro A, Mails Arad S. Complexes of Cu-polysaccharide of a marine red microalga produce spikes with antimicrobial activity. *Mar Drugs* 2022;20:787.
- [45] Hannauer M, Braud A, Hoegy F, Ronot P, Boos A, Schalk IJ. The PvdRT-OpmQ efflux pump controls the metal selectivity of the iron uptake pathway mediated by the siderophore pyoverdine in *Pseudomonas aeruginosa*. *Environ Microbiol* 2012;14:1696–708.
- [46] Yaniv K, Golberg K, Kramarsky-Winter E, Marks R, Pushkarev A, Bèjà O, Kushmaro A. Functional marine metagenomic screening for anti-quorum sensing and anti-biofilm activity. *Biofouling* 2017;33:1–13.
- [47] Golberg K, Markus V, Kagan B, Barzanzian S, Yaniv K, Teralki K, Kramarsky-Winter E, Marks RS, Kushmaro A. Anti-virulence activity of 3,3'-diindolylmethane (DIM): a bioactive cruciferous phytochemical with accelerated wound healing benefits. *Pharmaceutics* 2022;14:967.
- [48] Kanehisa M, Furumichi M, Sato Y, Kawashima M, Ishiguro-Watanabe M. KEGG for taxonomy-based analysis of pathways and genomes. *Nucleic Acids Res* 2023;51:D587–92.
- [49] Kanehisa M. Toward understanding the origin and evolution of cellular organisms. *Protein Sci* 2019;28:1947–51.
- [50] Kanehisa M, Goto S. KEGG: Kyoto Encyclopedia of genes and genomes. *Nucleic Acids Res* 2000;28:27–30.
- [51] Winsor GL, Griffiths EJ, Lo R, Dhillon BK, Shay JA, Brinkman FSL. Enhanced annotations and features for comparing thousands of *Pseudomonas* genomes in the *Pseudomonas* genome database. *Nucleic Acids Res* 2016;44:646.
- [52] Roy AB, Petrova OE, Sauer K. Extraction and quantification of cyclic di-GMP from *P. Aeruginosa*. *Bio Protoc* 2013;3:e828.
- [53] Heike Bähre VK. Identification and quantification of cyclic di-guanosine monophosphate and its linear metabolites by reversed-phase LC-MS/MS. *Methods Mol Biol* 2017;45–58.
- [54] Mirza Z, Walhout AJM, Ambros V. A bacterial pathogen induces developmental slowing by high reactive oxygen Species and mitochondrial dysfunction in *Caenorhabditis elegans*. *Cell Rep* 2023;42:113189.
- [55] Gallagher LA, Manoil C. *Pseudomonas aeruginosa* PAO1 kills *Caenorhabditis elegans* by cyanide poisoning. *J Bacteriol* 2001;183:6207–14.
- [56] Tan MW, Mahajan-Miklos S, Ausubel FM. Killing of *Caenorhabditis elegans* by *Pseudomonas aeruginosa* used to model mammalian bacterial pathogenesis. *Proc Natl Acad Sci U S A* 1999;96:715–20.
- [57] CDC. Antibiotic resistance threats in the United States, 2019. Atlanta, ga: U.S. Department of health and human Services, cdc; 2019. The biggest antibiotic-resistant threats in the U.S., 2019. Centers for Disease Control and Prevention; 2020.
- [58] Patriquin GM, Banin E, Gilmour C, Tuchman R, Greenberg EP, Poole K. Influence of Quorum sensing and iron on twitching motility and biofilm formation in *Pseudomonas aeruginosa*. *J Bacteriol* 2008;190:662–71.
- [59] Szklarczyk D, Kirsch R, Koutrouli M, Nastou K, Mehryary F, Hachilif R, Gable AL, Fang T, Doncheva NT, Pyysalo S, et al. The STRING database in 2023: protein-protein association networks and functional enrichment analyses for any sequenced genome of interest. *Nucleic Acids Res* 2023;51:D638–46.
- [60] Shannon P, Markiel A, Ozier O, Baliga NS, Wang JT, Ramage D, Amin N, Schwikowski B, Ideker T. Cytoscape: A software environment for integrated models of biomolecular interaction networks. *Genome Res* 2003;13:2498–504.
- [61] Barrientos-Moreno L, Molina-Henares MA, Ramos-González MI, Espinosa-Urgel M. Arginine as an environmental and metabolic cue for cyclic diguanylate signalling and biofilm formation in *Pseudomonas putida*. *Sci Rep* 2020;10:1–15.
- [62] Wellington S, Greenberg EP. Quorum sensing signal selectivity and the potential for interspecies cross talk. *mBio* 2019;10.
- [63] Haridevamuthu B, Seenivasan B, Priya PS, Muthuraman S, Kumar RS, Manikandan K, Almutairi BO, Almutairi MH, Arokiyaraj S, Gopinath P, et al. Hepatoprotective effect of dihydroxy piperlongumine in high cholesterol-induced non-alcoholic fatty liver disease zebrafish via antioxidant activity. *Eur J Pharmacol* 2023;945:175605.
- [64] Whitehead NA, Barnard AML, Slater H, Simpson NJL, Salmond GPC. Quorum-sensing in gram-negative bacteria. *FEMS Microbiol Rev* 2001;25:365–404.
- [65] Rasmussen TB, Bjarnsholt T, Skindersoe ME, Hentzer M, Kristoffersen P, Kôte M, Nielsen J, Eberl L, Givskov M. Screening for quorum-sensing inhibitors (QSI) by use of a novel genetic system, the QSI selector. *J Bacteriol* 2005;187:1799–814.
- [66] Rust L, Pesci EC, Iglewski BH. Analysis of the *Pseudomonas aeruginosa* elastase (lasB) regulatory region. *J Bacteriol* 1996;178:1134–40.
- [67] Duan X, Pan Y, Cai Z, Liu Y, Zhang Y, Liu M, Liu Y, Wang K, Zhang L, Yang L. rpoS-mutation variants are selected in *Pseudomonas aeruginosa* biofilms under imipenem pressure. *Cell Biosci* 2021;11:138.
- [68] Irie Y, Starkey M, Edwards AN, Wozniak DJ, Romeo T, Parsek MR. *Pseudomonas aeruginosa* biofilm matrix polysaccharide psl is regulated transcriptionally by RpoS and post-transcriptionally by RsmA. *Mol Microbiol* 2010;78:158–72.
- [69] Whiteley M, Parsek MR, Greenberg EP. Regulation of Quorum sensing by RpoS in *Pseudomonas aeruginosa*. *J Bacteriol* 2000;182:4356–60.
- [70] Ueda A, Wood TK. Connecting Quorum sensing, C-Di-GMP, pel polysaccharide, and biofilm formation in *Pseudomonas aeruginosa* through tyrosine phosphatase TpbA (PA3885). *PLoS Pathog* 2009;5:e1000483.
- [71] Thi MTT, Wibowo D, Rehm BHA. *Pseudomonas aeruginosa* biofilms. *Int J Mol Sci* 2020;21:8671.
- [72] Hentzer M, Wu H, Andersen JB, Riedel K, Rasmussen TB, Bagge N, Kumar N, Schembri MA, Song Z, Kristoffersen P, et al. Attenuation of *Pseudomonas aeruginosa* virulence by Quorum sensing inhibitors. *EMBO J* 2003;22:3803–15.
- [73] Mann EE, Wozniak DJ. *Pseudomonas* biofilm matrix composition and niche biology. *FEMS Microbiol Rev* 2012;36:893–916.
- [74] Sakuragi Y, Kolter R. Quorum-sensing regulation of the biofilm matrix genes (pel) of *Pseudomonas aeruginosa*. *J Bacteriol* 2007;189:5383–6.
- [75] Murakami K, Ono T, Viducic D, Somiya Y, Kariyama R, Hori K, Amoh T, Hirota K, Kumon H, Parsek MR, et al. Role of psl genes in antibiotic tolerance of adherent *Pseudomonas aeruginosa*. *Antimicrob Agents Chemother* 2017;61.
- [76] Phungmaung P, Mekjaroen J, Saisorn W, Chatsuwat T, Sompam P, Leelahavanichkul A. Rapid synergistic biofilm production of *Pseudomonas* and *Candida* on the pulmonary cell surface and in mice, a possible cause of chronic mixed organismal lung lesions. *Int J Mol Sci* 2022;23:9202.
- [77] Hassett DJ, Howell ML, Ochsner UA, Vasil ML, Johnson Z, Dean GE. An operon containing fumC and sodA encoding fumarase C and manganese superoxide dismutase is controlled by the ferric uptake regulator in *Pseudomonas aeruginosa*: Fur mutants produce elevated alginate levels. *J Bacteriol* 1997;179:1452–9.
- [78] Hassett DJ, Howell ML, Sokol PA, Vasil ML, Dean GE. Fumarase C activity is elevated in response to iron deprivation and in mucoid, alginate-producing *Pseudomonas aeruginosa*: cloning and characterization of fumC and purification of native fumC. *J Bacteriol* 1997;179:1442–51.
- [79] Banin E, Vasil ML, Greenberg EP. Iron and *Pseudomonas aeruginosa* biofilm formation. *Proc Natl Acad Sci U S A* 2005;102:11076–81.
- [80] Damron FH, Oglesby-Sherrouse AG, Wilks A, Barbier M. Dual-seq transcriptomics reveals the battle for iron during *Pseudomonas aeruginosa* acute murine pneumonia. *Sci Rep* 2016;6:39172.
- [81] Glick R, Gilmour C, Tremblay J, Satanower S, Avidan O, Déziel E, Greenberg EP, Poole K, Banin E. Increase in rhamnolipid synthesis under iron-limiting conditions influences surface motility and biofilm formation in *Pseudomonas aeruginosa*. *J Bacteriol* 2010;192:2973–80.
- [82] Bredenbruch F, Geffers R, Nimitz M, Buer J, Häussler S. The *Pseudomonas aeruginosa* quinolone signal (PQS) has an iron-chelating activity. *Environ Microbiol* 2006;8:1318–29.
- [83] Oglesby AG, Farrow JM, Lee J, Tomaras AP, Greenberg EP, Pesci EC, Vasil ML. The influence of iron on *Pseudomonas aeruginosa* physiology: a regulatory link between iron and Quorum sensing. *J Biol Chem* 2008;283:15558–67.
- [84] Chevalier S, Bouffartigues E, Bazire A, Tahriroui A, Duchesne R, Tortuel D, Maillot O, Clamens T, Orange N, Feuilloley MGJ, et al. Extracytoplasmic function sigma factors in *Pseudomonas aeruginosa*. *Biochim Biophys Acta Gene Regul Mech* 2019;1862:706–21.

- [85] Llamas MA, Mooij MJ, Sparrius M, Vandenbroucke-Grauls Christina MJ E, Ratledge C, Bitter W. Characterization of five novel *Pseudomonas aeruginosa* cell-surface signalling systems. *Mol Microbiol* 2008;67:458–72.
- [86] Leoni L, Orsi N, de Lorenzo V, Visca P. Functional analysis of PvdS, an iron starvation sigma factor of *Pseudomonas aeruginosa*. *J Bacteriol* 2000;182:1481–91.
- [87] Zheng P, Sun J, Geffers R, Zeng A. Functional characterization of the gene PA2384 in large-scale gene regulation in response to iron starvation in *Pseudomonas aeruginosa*. *J Biotechnol* 2007;132:342–52.
- [88] Gicquel G, Bouffartigues E, Bains M, Oxaran V, Rosay T, Lesouhaitier O, Connil N, Bazire A, Maillot O, Bénard M, et al. The extra-cytoplasmic function sigma factor SigX modulates biofilm and virulence-related properties in *Pseudomonas aeruginosa*. *PLoS One* 2013;8:e80407.
- [89] Xuan G, Lv C, Xu H, Li K, Liu H, Xia Y, Xun L. Sulfane sulfur regulates LasR-mediated Quorum sensing and virulence in *Pseudomonas aeruginosa* PAO1. *Antioxidants* 2021;10:1498.
- [90] Xuan G, Lü C, Xu H, Chen Z, Li K, Liu H, Liu H, Xia Y, Xun L. Sulfane sulfur is an intrinsic signal activating MexR-regulated antibiotic resistance in *Pseudomonas aeruginosa*. *Mol Microbiol* 2020;114:1038–48.